



Selective amplification of ipRGC signals accounts for interictal photophobia in migraine

Harrison McAdams^a, Eric A. Kaiser^b, Aleksandra Igdalova^b, Edda B. Haggerty^b, Brett Cucchiara^b, David H. Brainard^c, and Geoffrey K. Aguirre^{b,1}

^aDepartment of Neuroscience, Perelman School of Medicine, University of Pennsylvania, Philadelphia, PA 19104; ^bDepartment of Neurology, Perelman School of Medicine, University of Pennsylvania, Philadelphia, PA 19104; and ^cDepartment of Psychology, University of Pennsylvania, Philadelphia, PA 19104

Edited by Marlene Behrmann, Carnegie Mellon University, Pittsburgh, PA, and approved June 5, 2020 (received for review April 20, 2020)

Second only to headache, photophobia is the most debilitating symptom reported by people with migraine. While the melanopsin-containing intrinsically photosensitive retinal ganglion cells (ipRGCs) are thought to play a role, how cone and melanopsin signals are integrated in this pathway to produce visual discomfort is poorly understood. We studied 60 people: 20 without headache and 20 each with interictal photophobia from migraine with or without visual aura. Participants viewed pulses of spectral change that selectively targeted melanopsin, the cones, or both and rated the degree of visual discomfort produced by these stimuli while we recorded pupil responses. We examined the data within a model that describes how cone and melanopsin signals are weighted and combined at the level of the retina and how this combined signal is transformed into a rating of discomfort or pupil response. Our results indicate that people with migraine do not differ from headache-free controls in the manner in which melanopsin and cone signals are combined. Instead, people with migraine demonstrate an enhanced response to integrated ipRGC signals for discomfort. This effect of migraine is selective for ratings of visual discomfort, in that an enhancement of pupil responses was not seen in the migraine group, nor were group differences found in surveys of other behaviors putatively linked to ipRGC function (chronotype, seasonal sensitivity, presence of a photic sneeze reflex). By revealing a dissociation in the amplification of discomfort vs. pupil response, our findings suggest a postretinal alteration in processing of ipRGC signals for photophobia in migraine.

ipRGCs | melanopsin | migraine | photophobia

People find bright light uncomfortable and sometimes even painful. This experience of light-induced discomfort is exacerbated in numerous clinical conditions and can be debilitating (1). We refer here to discomfort from light as photophobia, which is typically manifest as a somatic sensation localized to the eyes or head (2). A common cause of photophobia is migraine (3). Photophobia is reported by 80 to 90% of individuals during a migraine attack (4–6), and 50% of individuals report it as their most burdensome symptom (7). Even between headaches, people with migraine have a lowered threshold for pain from light as compared with headache-free controls (Haf) (8–11).

The signals that ultimately result in photophobia presumably begin with photoreceptors in the eye. Under daylight conditions, the cone photoreceptors capture photons and relay signals via retinal ganglion cells to thalamic and brainstem targets (Fig. 1A). A subset of retinal ganglion cells expresses the photopigment melanopsin (12). These intrinsically photosensitive retinal ganglion cells (ipRGCs) are capable of responding to light without synaptic input (13). There is evidence from rodent studies that ipRGCs project to the somatosensory thalamus, where they innervate neurons that are also sensitive to dural stimulation carried by trigeminal afferents (14) (Fig. 1A). This finding offers a neural mechanism by which light stimulation creates somatic discomfort. The ipRGCs contribute to several other “reflexive” functions of vision as well, most notably photoentrainment of the circadian rhythm (15, 16) and control of pupil size (17–19).

The ipRGCs may play a role in human photophobia. People who have migraine and are also blind from inherited rod-cone degeneration experience photophobia during a headache (14), implicating spared ipRGCs as the source of this sensation. In people without visual impairment, Stringham and colleagues (20) found that shorter wavelengths of light (closer to the peak spectral sensitivity of the melanopsin photopigment) tend to produce greater discomfort in healthy observers (20). Studies that use narrow-band light stimuli, however, are limited in their ability to probe the specific contribution of melanopsin to photophobia in the intact visual system. This is due to the considerable overlap of the cone and melanopsin spectral sensitivity functions (Fig. 1B). Moreover, some classes of ipRGCs also receive input from the cones (13, 21–23). As a consequence, photophobia may result from both melanopsin and cone signals after their integration within ipRGCs. It is unknown how these photoreceptor classes are weighted and combined to produce photophobia and how this process might be altered in migraine.

In previous work, we have shown that carefully tailored modulations of the spectral content of light may be used to selectively target melanopsin or the cones (24, 25). Here, we examine the contribution of cone and melanopsin signals to visual discomfort, and to pupil responses, in people who have migraine

Significance

The melanopsin-containing intrinsically photosensitive retinal ganglion cells (ipRGCs) may contribute to photophobia in migraine. We measured visual discomfort and pupil responses to cone and melanopsin stimulation—the photoreceptor inputs to the ipRGCs—in people with and without migraine. We find that people with migraine do not differ from those without headaches in how cone and melanopsin signals are weighted and combined to produce visual discomfort. Instead, migraine is associated with amplification of ipRGC signals for discomfort. This effect of migraine upon ipRGC signals is limited to photophobia, as we did not find an enhancement of pupil responses or a change in other behaviors linked to ipRGC function. Our findings suggest a postretinal amplification of ipRGC signals for photophobia in migraine.

Author contributions: H.M., E.A.K., B.C., D.H.B., and G.K.A. designed research; H.M., A.I., and E.B.H. performed research; H.M., E.B.H., and G.K.A. analyzed data; and H.M., E.A.K., and G.K.A. wrote the paper.

Competing interest statement: E.A.K. has received royalties from a patent shared with Alder Biopharmaceuticals. The remaining authors declare that they have no relevant financial interests that relate to the research described in this paper.

This article is a PNAS Direct Submission.

Published under the PNAS license.

Data deposition: The raw data and analysis code are available through GitHub (<https://github.com/gkaguirrelab/melSquintAnalysis>).

¹To whom correspondence may be addressed. Email: aguirreg@upenn.edu.

This article contains supporting information online at <https://www.pnas.org/lookup/suppl/doi:10.1073/pnas.2007402117/-DCSupplemental>.

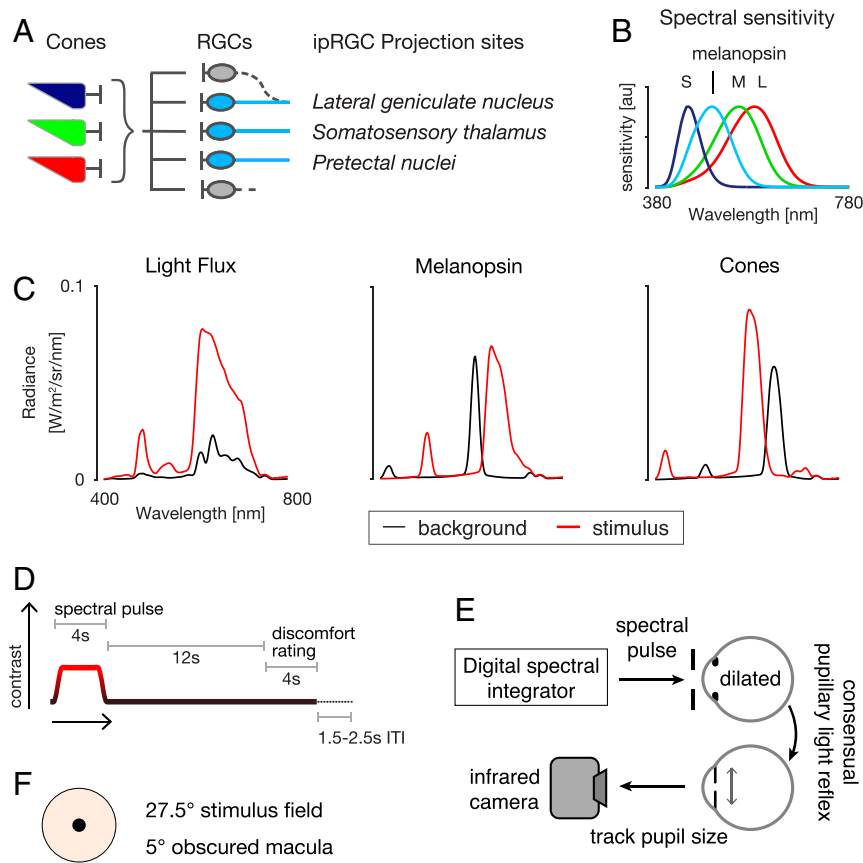


Fig. 1. Experiment overview. (A) There are several classes of melanopsin-containing ipRGCs, which vary in their central projections, function, and extent to which they receive input from cones. The ipRGCs project to the somatosensory thalamus and the lateral geniculate nucleus, where their signals may contribute to light sensitivity. Other ipRGCs project to the pretectal nuclei to control the size of the pupil. Not shown are numerous, additional subcortical projection targets of the ipRGCs (e.g., the suprachiasmatic nucleus). RGC, retinal ganglion cell. (B) The spectral sensitivity functions of the relevant photoreceptors under daylight conditions. S, M, and L refer to the short-, medium-, and long-wavelength sensitive cones, respectively. (C) Shown are pairs of spectra (background: black; stimulus: red) that differ in excitation for the targeted photoreceptors. In *Left*, *Center*, and *Right*, the stimuli produce equal contrast on the cones and melanopsin (termed light flux), contrast only on melanopsin, and equal contrast across all three classes of cones but no contrast on melanopsin, respectively. (D) Each trial featured a 4-s period during which the stimulus transitioned from the background to the stimulation spectrum and back. Twelve seconds after stimulus offset, the subject provided a discomfort rating. There was an intertrial interval that varied between 1.5 and 2.5 s. (E) The light from a digital spectral integrator was presented to the pharmacologically dilated right eye of the subject through an artificial pupil. The consensual pupillary light response of left eye was recorded with an infrared camera. (F) The stimulus spectra were presented in an eyepiece with a 27.5°-diameter field, with the central 5° obscured to minimize macular stimulation.

with interictal photophobia. Participants reported the discomfort they experienced from viewing pulses of light that selectively targeted melanopsin, the cones, or their combination (Fig. 1 C and D). Pupillometry in response to these pulses was also obtained (Fig. 1E). We recruited 20 participants in each of three groups: migraine with visual aura (MwA), migraine without aura (MwoA), and HAF. All of the participants with migraine endorsed interictal sensitivity to light. Our findings demonstrate that both melanopsin and cone stimulation in isolation produce visual discomfort. By examining the effect of separate and simultaneous stimulation of melanopsin and the cones, we quantified how these photoreceptor signals are weighted and combined to produce visual discomfort and pupil responses. We find that the enhanced interictal light sensitivity observed in migraine is well described as an amplification of photoreceptor signals after their combination. We further demonstrate that pupil responses are governed by different combination parameters and do not demonstrate amplification in migraine. These results indicate that interictal photophobia in migraine is a selective amplification of a subset of ipRGC outputs, most plausibly at a postretinal locus.

Results

Participant Demographic and Clinical Characteristics. We studied 20 people from each of three groups: MwA, MwoA, and HAF. The three groups (Table 1) were well matched in age ($F[2,57] = 0.2$, $P = 0.820$) but differed in gender distribution ($F[2,57] = 3.3$, $P = 0.0439$), with fewer women in the control group. The greater proportion of women in the migraine groups is consistent with migraine epidemiology (26). Headache frequency was similar in the two migraine groups with 12 (± 10) and 13 (± 9) days with headache reported within a 90-d period by MwA and MwoA subjects, respectively (approximately four headache days per month), consistent with a classification of episodic (as opposed to chronic) migraine (27). Acetaminophen and nonsteroidal anti-inflammatory drug (NSAID) use (for any indication) were similar across all three groups. Triptan use was reported by five MwA participants and one MwoA participant. Similarly, combined aspirin/acetaminophen/caffeine (Excedrin) use was reported by six MwA participants and one MwoA participant. Preventive medication use (e.g., tricyclics, beta-blockers, etc.) was reported by one MwA participant and three MwoA participants. We quantified headache disease burden using the Migraine Disability Assessment Test (MIDAS) (28) and Headache

Table 1. Subject demographic and clinical characteristics

Group	No. of women	Age (y)	Headache days/3 mo	Disability		Medication use last 3 mo				
				MIDAS	HIT-6	NSAID	Actmnpn	Excedrin	Triptan	Preventive
Controls	13/20	31 (5)	1.3 (1.4)	0.5 (0.8)	40.7 (4.1)	14	1	0	0	0
MwA	19/20	31 (4)	13.1 (8.9)	18.6 (15.3)	60.6 (8.0)	16	5	6	5	1
MwoA	17/20	30 (4)	11.7 (9.7)	16.0 (13.7)	60.0 (8.8)	17	2	1	1	3

Participants were asked to report the number of headaches they had experienced over the prior 3 mo. The MIDAS (28) and the HIT-6 (29) measure headache disability. Where appropriate, the mean value (and SD) across subjects is reported. Medication use is summarized within five categories: actmnpn, acetaminophen for any indication; Excedrin, use of any one of multiple formulations that combine an NSAID with acetaminophen to treat headache; NSAID, NSAID for any indication; preventive, any one of several classes of medications used to decrease migraine frequency (e.g., tricyclic antidepressants, beta-blockers); triptan, any tryptamine-based drug used to abort a migraine.

Impact Test (HIT-6) (29) surveys. The migraine groups unsurprisingly had higher scores on both instruments relative to HAF (MIDAS: $F[2,57] = 13.65$, $P = 1.43e-5$; HIT-6: $F[2,57] = 48.82$, $P = 4.43e-13$). The two migraine groups did not differ in disease impact (MIDAS: $t = 1.00$, $P = 0.76$; HIT-6: $t = 0.40$, $P = 0.96$). The distribution of these values suggests moderate disability from migraine in both groups.

Participants with Migraine Have Interictal Photophobia but Do Not Differ from Controls in Surveys of Circadian and Seasonal Behavior.

The Visual Discomfort Scale (VDS) measures symptoms of discomfort from reading, patterns, and light on a 0 to 69 scale (30). We required our control participants to have a low score on this instrument (less than or equal to seven) but did not impose a requirement for migraineurs. Symptoms of visual discomfort were correspondingly greater in the migraine population as compared with the controls (Table 2) ($F[2,57] = 15.23$, $P = 5.02e-6$). Participants also completed the Photosensitivity Assessment Questionnaire (PAQ), which measures light-avoiding (“photophobia”) and light-seeking (“photophilia”) behavior on a zero to eight scale (31). Migraine participants again reported greater light avoidance as compared with controls (Table 2) ($F[2,57] = 10.95$, $P = 9.44e-5$), although there was no difference in reported light-seeking behavior (Table 2) ($F[2,57] = 0.75$, $P = 0.448$).

As we are interested in how migraine and photophobia may relate to ipRGC function, we examined if our participant groups differed in other functions thought to be mediated by ipRGCs. In the rodent, multiple classes of ipRGCs have been identified that differ in their subcortical projections and in their functional properties. Projections of the ipRGCs to the suprachiasmatic nucleus are thought to control circadian photoentrainment (15). As variation in this function is speculated to relate to sleep alterations and seasonal affective disorder, we gathered information about the sleep habits and seasonal preferences of our participants (Table 2). The Morningness-Eveningness Questionnaire (32) characterizes chronotype on a scale of 16 to 86, with the extremes corresponding to evening and morning preference, respectively. The median scores for the three groups all

were in the midrange (~50) and were not significantly different ($F[2,57] = 0.54$, $P = 0.586$). The Seasonal Pattern Assessment Questionnaire (33) provides a Global Seasonality Score, which assesses on a 0 to 24 scale the degree to which mood and physiology vary across seasons; a score of 16 or higher is typical in patients with seasonal affective disorder. The central tendency of our participants (a score of approximately seven) indicates a mild degree of seasonal sensitivity, and this did not differ between the groups ($F[2,57] = 2.19$, $P = 0.121$). Finally, the photic sneeze reflex has been hypothesized to be related to ipRGC function (34), as the somatic “prickling” sensation of the nose in response to a bright light is suggestive of a retinotrigeminal interaction. We asked our participants if they experience this phenomenon and did not find any difference between groups in the proportion of participants (15 to 20%) who have this experience ($F[2,57] = 0.04$, $P = 0.962$).

Overall, apart from photophobia, our studied populations were well matched in behaviors hypothesized to be related to ipRGC function.

Melanopsin and Cone Contrast Produce Mild Discomfort in Control Participants.

Our participants rated the degree of discomfort they experienced while viewing pulses of spectral change that targeted melanopsin, the cones, or combined stimulation of both sets of photoreceptors (termed light flux). The stimuli were designed to increase excitation in the targeted photoreceptor(s) by 100, 200, or 400%. Participants rated the amount of discomfort produced by each type of light pulse on a 0 (none) to 10 (extreme) scale.

The light flux stimulus combines melanopsin and cone stimulation. In the HAF participants, light flux pulses evoked mild discomfort, increasing with contrast, reaching a mean discomfort rating of 3.15 of 10 for 400% contrast (Fig. 2, *Top Left*). To determine whether this discomfort was a consequence of melanopsin or cone-based signaling, we examined the discomfort ratings in response to stimuli designed to target these photoreceptor classes in isolation. Discomfort ratings to both melanopsin (Fig. 2, *Middle Left*) and cone-directed stimuli (Fig. 2, *Bottom Left*) also increased with contrast but only with mild discomfort at 400% (Fig. 2, *Middle Left* [mean rating of 2.18 for melanopsin]

Table 2. Surveys of behaviors that may be related to ipRGC function

Group	VDS	PAQ–photophobia	PAQ–photophilia	SPAQ	Morningness-Eveningness	Photic sneeze reflex
Controls	3.45 (1.76)	0.15 (0.19)	0.71 (0.21)	6.10 (3.81)	51.55 (10.28)	4
MwA	16.55 (10.00)	0.46 (0.28)	0.65 (0.22)	8.90 (5.53)	48.80 (10.53)	3
MwoA	13.15 (8.88)	0.51 (0.31)	0.63 (0.23)	8.65 (4.55)	48.75 (8.32)	3

The VDS measures reported light sensitivity across several domains of visual function (30). The PAQ measures reported photophobia and photophilia behaviors (31). The Seasonal Pattern Assessment Questionnaire (SPAQ) measures the reported degree to which mood and behavior vary over course of a year (33), and the Morningness-Eveningness Questionnaire provides a “chronotype” score (32). Values are the mean (and SD) across subjects within each group. Finally, we asked subjects if they “tend to sneeze when [they] step out of a dark room into bright sunlight” and report here the number of subjects in each group who responded “yes.”

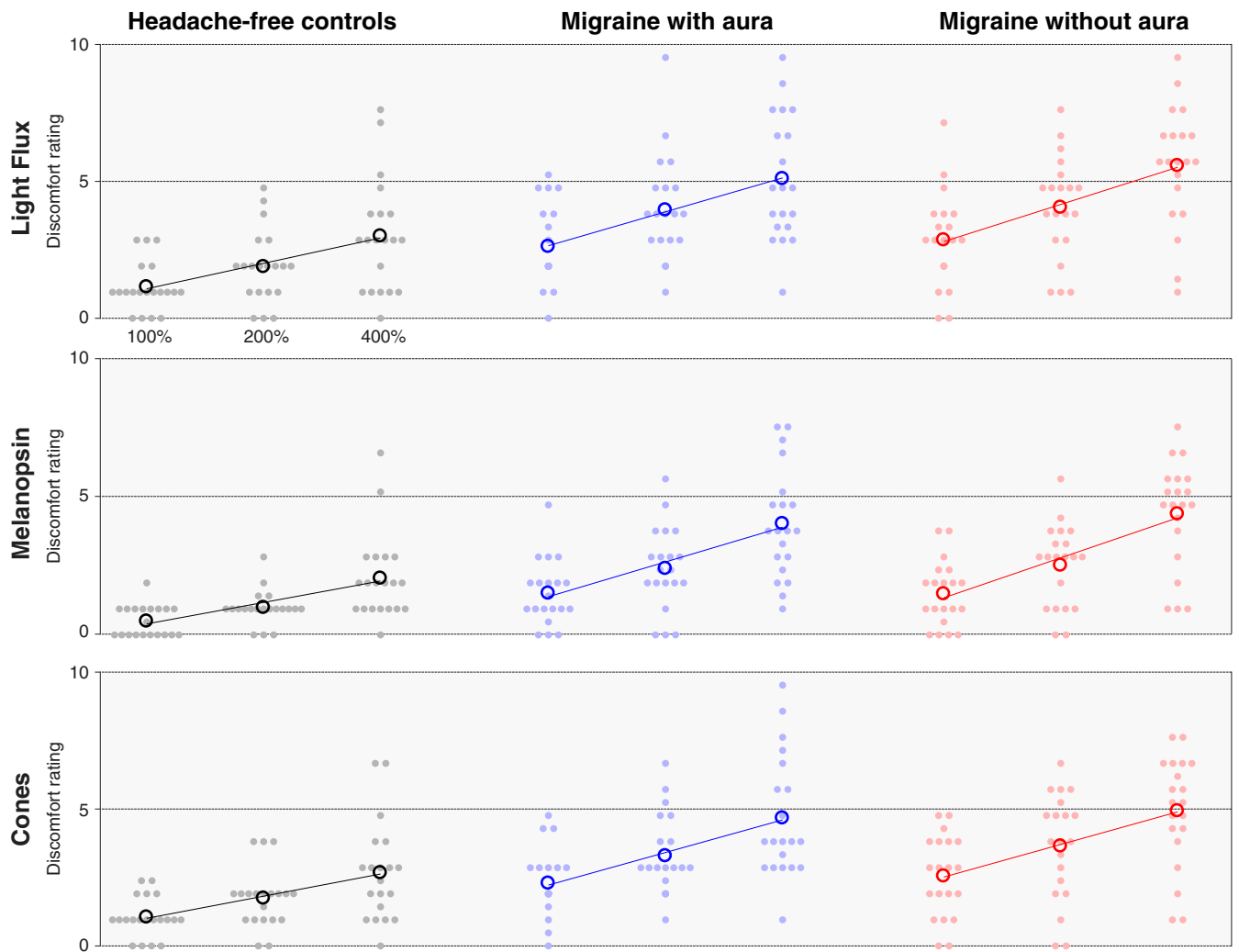


Fig. 2. Discomfort ratings by stimulus and group. Each row presents the discomfort ratings elicited by stimuli that targeted a particular combination of photoreceptors, and each column contains the data from each individual group ($n = 20$ participants per group). The stimuli were presented at three different contrast levels (100, 200, and 400%), and these (log-spaced) values define the x axis of each subplot. The median (across trial) discomfort rating for a given stimulus and contrast is shown for each participant (filled circles), as is the mean rating across participants (open circles). The best-fit line to the mean discomfort rating across participants as a function of log contrast is shown in each subplot.

and *Bottom Left* [2.80 for cones]). This result suggests that both cone and melanopsin signals contribute to light-induced discomfort. For all stimuli, we further observed that logarithmic changes in stimulus contrast produced linear changes in mean rated discomfort, as illustrated by the good agreement between the fit lines and the data (Fig. 2).

Cone and Melanopsin Signals Contribute to Interictal Photophobia in Migraine. We next asked if people with photophobic migraine would experience greater discomfort in response to our stimuli and if so, whether the enhanced discomfort signal is attributable to the cones, melanopsin, or both. Both migraine groups showed increased discomfort in response to the combined light flux stimuli at all contrast levels (Fig. 2, *Top Center* and *Top Right*: at 400% contrast, mean of 5.35 for MwA and 5.85 for MwoA vs. 3.15 for controls). The mean rating across participants was also increased in both migraine groups in response to melanopsin-directed stimulation (Fig. 2, *Middle*: at 400% contrast, mean of 4.28 for MwA and 4.65 for MwoA vs. 2.18 for controls) and cone-directed stimulation (Fig. 2, *Bottom*: at 400% contrast, mean of 4.90 for MwA and 5.18 for MwoA vs. 2.80 for controls). Both

migraine groups also showed a linear relationship between log-spaced contrast and mean discomfort ratings for all stimulus types, which is again illustrated by the fit lines (Fig. 2). A mixed effects ANOVA confirmed that discomfort ratings were higher for all stimuli in the migraine groups as compared with the control group (*SI Appendix, Table S2*).

There was a higher proportion of women in the migraine groups as compared with the control group. We considered if this unequal distribution of gender could account for the differences in discomfort ratings between the groups. The mean discomfort rating reported by female control participants (across all stimuli) was not higher than the ratings provided by male participants (mean rating men: 1.79; women: 1.74), indicating that differing gender ratios do not account for the increased discomfort in the migraine groups.

Discomfort Ratings Are Well Fit by a Two-Stage, Nonlinear, Log-Linear Model. We observe that mean discomfort ratings for all stimuli are well described as a linear function of log-scaled stimulus contrast, consistent with the Weber–Fechner law of perception. It is also apparent that a light flux stimulus, which combines

melanopsin and cone contrast, evokes less discomfort than would be predicted given the discomfort produced by each stimulus component alone. These properties of the data may be explained by nonlinear combination of melanopsin and cone signals prior to the stage at which photoreceptor signals are interpreted as discomfort.

We examined these impressions within the context of a quantitative, two-stage model governed by four parameters. The first stage is based upon psychophysical measures of combined stimulus dimensions (35, 36), and the second is on the Weber–Fechner law. The model provides a discomfort rating for stimuli with arbitrary combinations of melanopsin and cone contrast.

The first stage of the model (Fig. 3 *A, Left*) considers the combination of melanopsin and cone signals within ipRGCs. The inputs to this stage are the contrasts on the melanopsin and cone photoreceptors created by a stimulus. A light flux stimulus of (for example) 200% contrast has the property of providing 200% contrast input on both of these photoreceptor classes. A scaling factor (α) adjusts the relative potency of melanopsin contrast as compared with cone contrast. The two contrast types are then combined using a Minkowski distance metric with exponent β .

This integrated “ipRGC contrast” is log transformed and then passed to the second stage of the model (Fig. 3 *A, Right*), which transforms input into a discomfort rating under the control of a slope and offset parameter (which is the intercept transformed to describe the modeled response to 200% contrast).

We fit this model to the discomfort ratings across trials for all stimuli and participants within a particular group using bootstrap resampling across participants to characterize the variability of the model parameters. Fitting was performed separately for the data from each group (Fig. 3*B*). The model performed equally well for each group in accounting for the mean (across-participant) discomfort ratings across stimuli (model $R^2 \pm$ SEM: HAF: 0.95 ± 0.03 ; MwA: 0.96 ± 0.03 ; MwoA: 0.97 ± 0.01).

Migraine Groups Differ from HAF in the Response to Integrated Melanopsin and Cone Signals. We examined the fitted parameters of the model and compared these values across groups (Fig. 3*B*). The discomfort data from all three groups are best fit by first scaling (α) the influence of melanopsin contrast by $\sim 60\%$. The scaled melanopsin and cone contrast are then combined with a subadditive Minkowski exponent (β) of ~ 1.75 , intermediate between

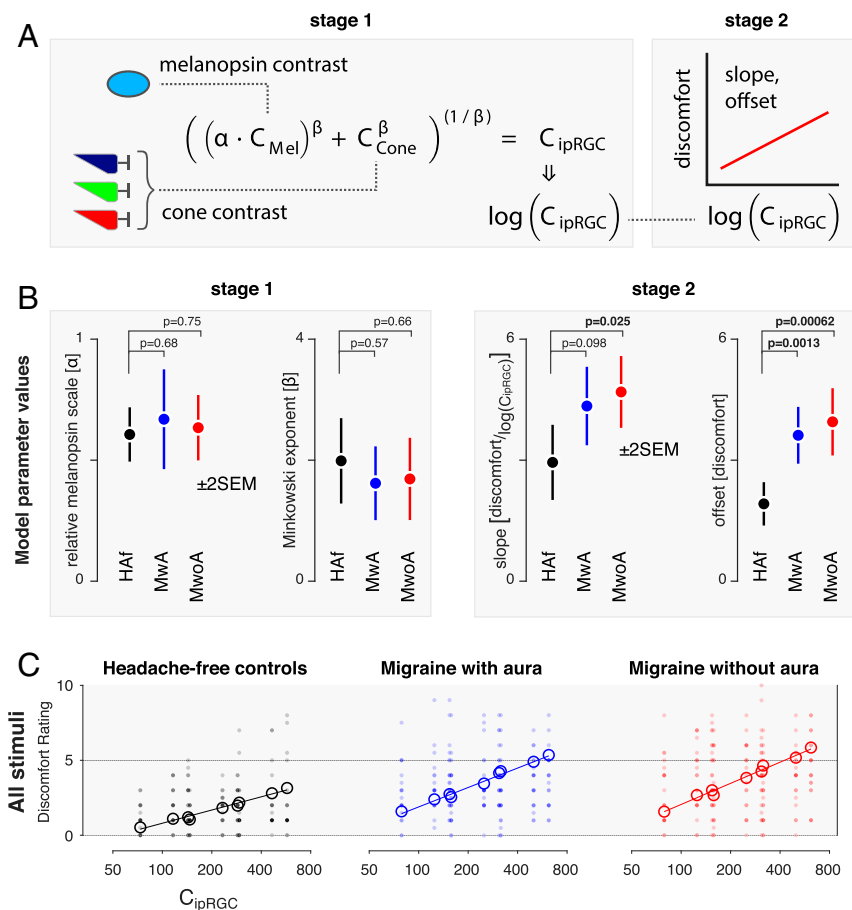


Fig. 3. A two-stage model of discomfort ratings. We developed a two-stage model that describes discomfort ratings as a function of melanopsin and cone stimulation. (*A*) In the first stage, (*Left*) melanopsin contrast (C_{Mel}) is weighted by a scaling factor (α) and then combined with cone contrast (C_{Cone}) under the control of the Minkowski exponent (β). The output of this stage is ipRGC contrast, which is log transformed and passed to the second stage (*Right*). Here, the signal undergoes an affine transform to produce a discomfort rating, under the control of a slope and offset parameter (the latter being expressed as the modeled discomfort rating at 200% ipRGC contrast). (*B*) The model was fit to the discomfort data from each group, yielding estimates of the model parameters (± 2 SEM obtained via bootstrapping). The P value associated with a two-tailed t value, taken with respect to the pooled SEs, is presented for the comparison of each of the migraine groups with the control group for each parameter ($n = 20$ participants per group). (*C*) Stage 1 of the model transforms the stimuli used in the experiment to common units of ipRGC contrast. Each plot presents the discomfort ratings (individual participants in filled circles, group means in open circles) in terms of ipRGC contrast, with the parameters at stage 1 forced to be the same across groups. The nine open circles correspond to the nine stimuli used in the experiment (three contrast levels each of melanopsin, cone, and light flux stimulation). The fit of the second stage of the model (which can vary across groups) provides the fit line.

simple additivity ($\beta = 1$) and a Euclidean distance metric ($\beta = 2$). We find that these parameter values do not significantly differ between the three groups (Fig. 3 B, *Left*). Therefore, we do not find that people with photophobic migraine differ from HAF in the manner in which melanopsin and cone signals are combined at this initial stage.

The second pair of parameters converts log-transformed ipRGC contrast into discomfort ratings. Here, substantial differences between the migraine and control groups were found. The MwoA group had a greater slope and a higher offset of discomfort rating, and the Mwa group had a higher offset, for a given amount of ipRGC contrast (Fig. 3 B, *Right*). The migraine groups reported discomfort that was roughly twice as great overall and had a slope that was 50% steeper as compared with controls for the increase in discomfort with ipRGC contrast.

Based upon these results, we refit the model, forcing the stage 1 parameters to be the same across the three groups but allowing the stage 2 parameters to vary. The output of stage 1 allows us to describe all of the stimuli used in the experiment in terms of a single value of ipRGC contrast. Fig. 3C replots the discomfort data for all participants and all stimuli from each group in terms of the stage 1 value of ipRGC contrast. The stage 2 model fits differ for each group and are used to generate the solid lines on the plots. Open circles mark the mean, across-participant discomfort ratings for each of the nine stimulus types. There is good agreement between the model fit and the across-participant mean discomfort. Forcing the stage 1 parameters to be the same across groups had minimal impact upon the fit of the model to the data (model $R^2 \pm \text{SEM}$: HAF: 0.95 ± 0.03 ; Mwa: 0.96 ± 0.02 ; MwoA: 0.97 ± 0.01), supporting the claim that the stage 1 model parameters do not meaningfully differ between the groups.

Overall, these findings indicate that people with migraine with interictal photophobia do not differ from controls in the manner in which cone and melanopsin signals are scaled relative to each other and combined but experience greater discomfort from this integrated signal.

Migraine Groups Do Not Have Enhanced Pupil Responses, Indicating a Selective Enhancement of ipRGC Discomfort Signals. We considered the possibility that people with migraine have a general amplification of ipRGC signals at the level of the retina, of which visual discomfort is one aspect. If so, then we might expect an amplification of pupil responses to be seen in this population as well. To test this idea, we compared pupil constriction in the migraine groups with that observed in the HAF participants.

Fig. 4A presents the mean, across-participant pupil responses observed in each of the three groups to the stimuli used in the experiment. The temporal profile of the pupil response to stimuli that target melanopsin, the cones, or their combination is in good agreement with prior reports (25). There is also a clear increase in the amplitude of the pupil constriction produced by stimuli with increasing (100, 200, 400%) contrast.

The responses obtained from each studied group are close to overlapping in the plots for each combination of stimulus direction and contrast. We did not observe a greater amplitude of pupil response in the migraine groups as compared with the controls. Indeed, if anything, the pupil response in the migraine groups (particularly MwoA) is slightly attenuated compared with that of the HAF. We quantified the pupil response for each participant by measuring the mean percent change in pupil area following stimulus onset (*SI Appendix*, Fig. S1). Similar to what was observed for visual discomfort ratings, the relationship between pupil response and stimulus contrast is well described as log linear.

We next examined how cone and melanopsin signals are combined to produce the overall amplitude of pupil constriction, using the same two-stage model that we developed for the discomfort ratings (Fig. 4B). The model fit the data from the three

groups well (model $R^2 \pm \text{SEM}$: HAF: 0.95 ± 0.03 ; Mwa: 0.98 ± 0.01 ; MwoA: 0.94 ± 0.02). We found no significant differences between the groups in the parameters of the model for pupil response. Therefore, we refit the model to the pupil data, forcing all parameters to be the same across the groups (Fig. 4C). The agreement between the data and the model was quite good, despite requiring that all three groups be described using the same model parameters (model $R^2 \pm \text{SEM}$: HAF: 0.96 ± 0.01 ; Mwa: 0.95 ± 0.001 ; MwoA: 0.91 ± 0.06).

The stage 1 parameters in control of the pupil describe a scaling factor for melanopsin (α) of ~40%, which is somewhat less than the influence that melanopsin has upon discomfort (~60%). The Minkowski exponent for the combination of melanopsin and cone signals in the pupil response is ~0.8, compared with its value of ~1.75 for the discomfort ratings. The value of ~0.8 indicates a combination rule for cone and melanopsin signals that is reasonably close to linear, consistent with prior observations of the additivity of cone and melanopsin signals in the pupil response (24, 37). The fact that the stage 1 parameters differ between the model fits to the two measures indicates that discomfort and pupil control are mediated by mechanisms that combine signals from melanopsin and the cones in different ways. A possible neural basis for these mechanisms would be distinct classes of ipRGCs.

Separately from the matter of how signals from melanopsin and the cones are combined across the two measures, the fact that the stage 2 parameters differ between controls and people with migraine for the production of discomfort but not for pupil constriction argues against the idea that a common, single amplification of retinal signals mediates increased interictal photophobia in migraine.

Discussion

Our study indicates that the enhanced, interictal light sensitivity experienced by people with migraine is due to a selective amplification of response to a subset of ipRGC signals. Photophobia in migraine is not the result of an omnibus change in cone or melanopsin signals per se but instead, a change in the response to these photoreceptor inputs after they have been weighted and combined. Moreover, this enhanced response is specific for discomfort signals in that it is not observed for ipRGC outputs that control other reflexive responses to light, in particular pupil constriction.

Distinct ipRGC Classes. Studies in rodents (38–40), primates (13, 41–43), and in the postmortem human eye (44, 45) have demonstrated the existence of multiple classes and subclasses of ipRGCs, which differ in their photoreceptor inputs, signaling kinetics, and central projections. Control of circadian photoentrainment and the pupil response, for example, is attributable to distinct subsets of ipRGCs in rodents (38, 46).

We examined how melanopsin and cone inputs contribute separately and in combination to visual discomfort and to the pupil response within the context of a quantitative model. The first stage of our model estimates how melanopsin signals are weighted relative to cone signals and the metric with which melanopsin and cone signals are combined. We did not find a difference at this stage between people with or without migraine. We did find, however, that the model parameters differ substantially when measured for the pupil response and for ratings of visual discomfort. A plausible explanation for these differences in photoreceptor combination is that different classes of ipRGCs contribute to visual discomfort and pupil responses in the human.

In the current study, we find that melanopsin and cone signals are combined approximately additively in control of the pupil, consistent with prior reports (24, 37). Melanopsin contrast was 40% as effective as cone contrast in modulating the pupil for

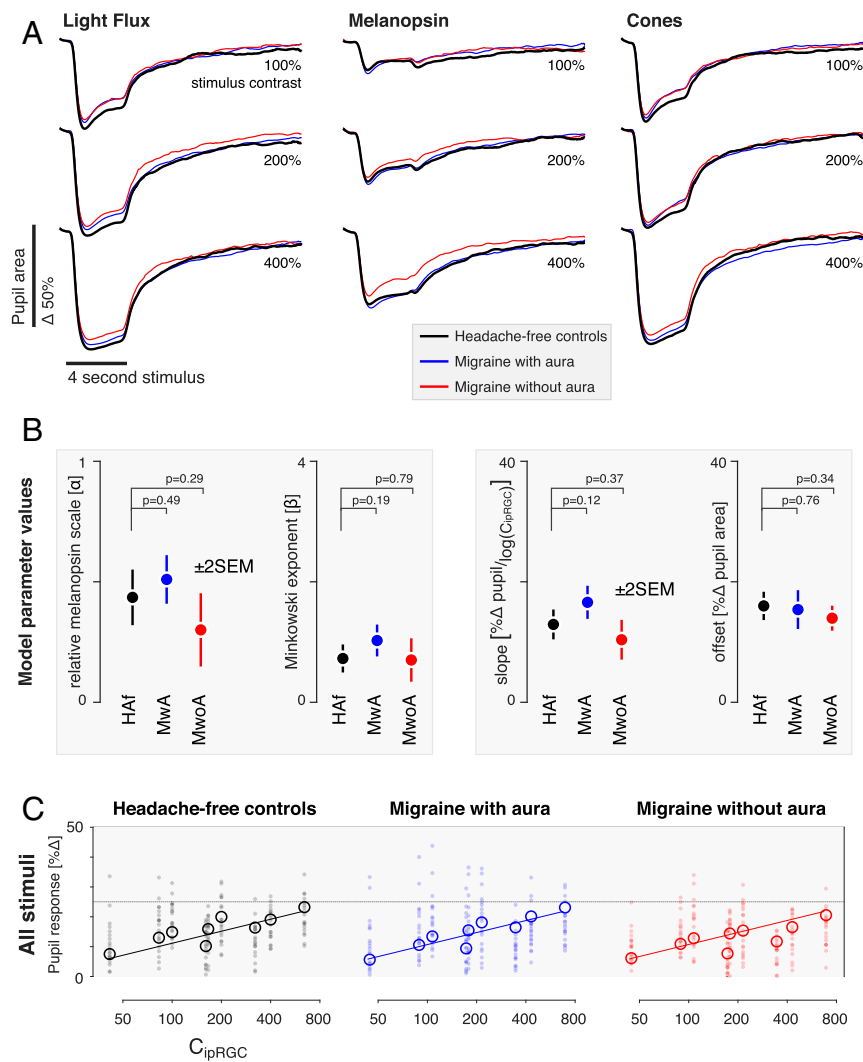


Fig. 4. Pupil response by stimulus and group. (A) The average pupil response across participants within each group ($n = 20$ participants per group) is shown for each stimulus type (columns) at each contrast level (rows). The responses from the three groups for each stimulus type are superimposed. (B) We summarized the pupil responses by taking the mean of the percent change in amplitude of the pupil area across the recording period. These data were then fit with the two-stage model (Fig. 3). No significant differences between the groups in the parameter estimates were found (± 2 SEM obtained via bootstrapping), although both the relative melanopsin scaling and Minkowski exponent values are smaller for pupil responses than was observed for discomfort ratings. (C) As no significant differences between groups were found for the parameters, we refit our model to the data forcing all parameters to be the same across groups. The plots report individual (filled circles) and mean (open circles) pupil response as a function of modeled ipRGC contrast.

these pulsed stimuli, as compared with a prior report of an overall 26% effectiveness of melanopsin relative to modulations that placed equal contrast on long- and medium-wavelength sensitive cones for driving pupil responses with sinusoidal modulations of contrast at low and high temporal frequencies (24). We note that our index of pupil change here was across the entire time course of evoked response. While it is likely that the relative contribution of melanopsin to the amplitude of pupil constriction varies as a function of time following stimulus onset (19, 25, 37, 47, 48), such a dissection of the components of the pupil response is beyond the scope of the current report.

In contrast to the pupil response, melanopsin and cone signals exhibit a nearly Euclidean combination metric in our measure of discomfort, and we find that the influence of melanopsin signals (relative to the cones) is ~ 1.5 times greater in producing visual discomfort as compared with pupil responses. A Euclidean combination metric is a feature of stimulus dimensions that produce a single, integrated percept (35), suggesting that cone

and melanopsin signals are combined into a unitary experience of discomfort.

We have previously found that observers describe targeted melanopsin stimulation as “uncomfortable brightness” (49). It may be the case that the “brightness” and “discomfort” percepts, while each integrating cone and melanopsin signals, reflect the action of distinct retinal ganglion cell populations. Our present data, however, do not directly address such a dissociation.

Several studies have demonstrated that melanopsin contrast contributes to a sensation of brightness (50–53). The melanopic component of brightness is presumably combined with the postreceptoral luminance channel that is derived from the sum of L and M cone excitations and carried by the classical (nonmelanopsin-containing) retinal ganglion cells. Yamakawa and colleagues (51) measured the perceptual brightness of lights that varied in melanopic and luminance content. A roughly additive effect of luminance and melanopsin content upon brightness is present in their data, although the form of the response

departed from linear. The interpretation of these measurements is complicated, however, as the observers did not undergo pharmacologic dilation of the pupil, causing retinal irradiance to vary systematically with the stimulus.

Zelevansky and colleagues (53) also examined how cone and melanopsin signals combine in the perception of brightness. Their work shows a log-linear relationship between isolated melanopsin and cone stimulus intensity and brightness. However, when presented in combination, they report two contribution components of cones to brightness, one of which is negative and may imply an adaptation process.

Selective Amplification. The ipRGCs are known to manifest linear changes in firing rates with logarithmic changes in retinal irradiance (54). In our measurements, we find that ratings of visual discomfort and the amplitude of evoked pupil response vary linearly with log changes in stimulus contrast, consistent with an output system that receives these log-transformed signals from the ipRGCs.

While participant groups did not differ in the manner in which cone and melanopsin signals were combined, we find that people with episodic migraine with interictal photophobia have an enhanced response to this integrated signal in their ratings of visual discomfort. This amplification is similar in migraine with or without visual aura.

Importantly, we did not find evidence of a general amplification of ipRGC signals in migraine. The ipRGCs are the dominant, and perhaps exclusive, route for photoreceptor signals influencing the light-evoked pupil response via the pretectal nuclei (55, 56). If migraine is accompanied by a general amplification of ipRGC signals, then an enhanced light-evoked pupil response in this population might be predicted. Instead, we find that the amplitude of evoked pupil responses is not increased in people with migraine in response to stimulation of melanopsin, the cones, or their combination. Indeed, the trend in the data was toward smaller evoked pupil responses in migraine, especially in MwoA. Prior studies of pupil response in migraine have obtained varying results. Prior studies have not found migraine group differences in the amplitude of pupil constriction or steady-state pupil size (57–60), although more subtle changes in pupil dynamics have been reported (58, 61, 62). Our study differs from many prior reports in that we measured open-loop, consensual pupil responses by combining pharmacologic dilation with an artificial pupil, thus controlling retinal irradiance across the studied groups.

We also surveyed our participants regarding other behaviors that may be related to ipRGC function. A general alteration in ipRGC function in people with migraine might be predicted to be manifest in these measures as well. The ipRGCs have been implicated in circadian photoentrainment (15), seasonal variation in mood and physiology (63–65), and in the photic sneeze reflex. Our participants with migraine did not differ from HAF in these behaviors, again suggesting that the amplification of ipRGC signals in migraine is specific to visual discomfort.

The Neural Locus of Amplification. While no specific ipRGC subtype has been identified as carrying the signal for visual discomfort, various lines of evidence implicate ipRGCs distinct from the M1 subtype (66–68). The ipRGCs coinnervate neurons within the posterior thalamus of the rodent that also receive trigeminal afferents. These thalamic neurons then project onward to both somatosensory and visual cortices. Classes of ipRGCs also project to the lateral geniculate nucleus (13, 54) and are capable of modulating visual cortex responses (49). Our findings of amplified discomfort to visual stimulation in people with migraine could reflect alteration of signals derived from the ipRGCs at any one of these sites.

A physiologic hallmark of migraine is alteration in the excitability of cortex, as manifest both in the phenomenon of cortical spreading depression of aura and a tendency toward enhanced responses to sensory stimulation as compared with HAF (69). Enhanced cortical responses to sensory stimulation have been observed in migraine with (69) and possibly without (70) aura, and for multiple sensory modalities. A natural locus, therefore, for the amplification of ipRGC signals for visual discomfort is at cortical sites. This could take place within primary visual or somatosensory cortex or further downstream at the point where multimodal signals are integrated into a report of discomfort.

An ipRGC signal of visual discomfort might also be amplified at the level of the thalamus. Altered thalamic gating has been proposed as a mechanism for altered sensory perception in migraine, including photophobia (3, 71). Enhanced signaling within the trigeminal system may also contribute to amplification of ipRGC signals. In rodents, bright light activates the trigeminal ganglion and trigeminal nucleus caudalis (72–74). Human studies suggest an interaction of the peripheral trigeminal system and light-mediated pathways as noxious trigeminal stimulation lowers the visual discomfort threshold, and light stimulation lowers trigeminal pain thresholds (11, 75). Studies in the rodent implicate the ipRGCs in this interaction as light aversion following corneal surface damage is attenuated in mice lacking ipRGCs (76). Migraine may induce photophobia through the action of neuropeptides within this trigeminal–thalamic system (77).

We might finally consider the possibility that ipRGC signals for visual discomfort are amplified at the level of the retina. This possibility strikes us as less plausible, given that our results would require a mechanism for selective enhancement of only the class of ipRGC that produces photophobia. Our results also argue against a change in the sensitivity of melanopsin or the cones in migraine under photopic conditions.

There have been varying reports of alteration of cone electroretinogram responses in people with migraine (78, 69), although these studies are also difficult to interpret given possible differences in retinal irradiance between the studied groups (80).

We interpret our results within a modeling approach that assumes that melanopsin and cone signals are integrated within the ipRGCs and that postretinal sites act upon the integrated, log-transformed signal. While this model was not a component of our preregistered experimental protocol, we find that it provides an excellent account of the data. There is abundant evidence in support of the view that melanopsin and cone signals are integrated in the ipRGCs (13, 21–23, 81). We cannot, however, exclude the possibility that cone and melanopsin signals are transmitted from the retina by separate channels and that we are measuring the integration of these signals at some downstream site. Such a postretinal integration is likely to be the case for the percept of brightness—which combines melanopsin and cone contrast—as the postretinal luminance channel originates in signals from the “classical” retinal ganglion cells and must be integrated with signals from melanopsin-containing ipRGCs, perhaps at the level of the lateral geniculate nucleus.

More broadly, there is evidence that expression of melanopsin in eye tissues apart from the retina contributes to photophobia in rodent models (34). Because we placed an artificial pupil between the stimulus and the pharmacologically dilated pupil of the observer, our stimuli illuminated only a small area of the cornea and minimally, the iris. There has also been interest in the contribution of the rods to photophobia in migraine (79), and there is evidence that the rods provide inputs to ipRGCs (82). We sought to minimize the influence of the rods upon our measurements by modulating our stimuli around a photopic background. While there is evidence that rod signals can modulate retinal ganglion cell firing at any light level (83), the amplitude of these effects under photopic conditions is quite small relative to the cones. Further, our prior work indicates that rod

signals do not make a measurable contribution to the pupil response at these background light levels (25).

Conclusion

Our study demonstrates that discomfort from light does not arise as the exclusive action of melanopsin but instead, reflects a signal that integrates cone and melanopsin inputs. The interictal photophobia of migraine is a selective amplification of this integrated signal and one that does not extend to other domains of ipRGC function. We suspect that the enhanced response in migraine to ipRGC signals for discomfort occurs at a postretinal site but cannot yet identify the locus. The modeling approach we adopted here provides a mechanism by which this localization might be pursued, by identifying central sites in which log changes in modeled ipRGC contrast are related to linear modulations of neural activity.

Materials and Methods

We studied 20 participants in each of three groups: MWA, MwoA, and HA (Table 1). Participants were between 25 and 40 y old and were recruited via digital social media. Headache classification was established using the Penn Online Evaluation of Migraine, which implements the International Classification of Headache Disorders-3-beta criteria (84). Participants with migraine were also required to endorse interictal photophobia (85). Participants completed surveys that assessed behaviors putatively related to ipRGC function (Table 2).

Participants viewed stimuli that targeted specific photoreceptor classes using the technique of silent substitution (86) (Fig. 1C). Each stimulus type was presented at three log-spaced contrast levels: 100, 200, and 400%. These stimuli were produced by a digital light synthesis engine (OneLight Spectra) and tailored for the lens transmittance predicted for the age of each subject. The stimuli were presented through a custom-made eyepiece with a circular, uniform field of 27.5° diameter with the central 5° diameter of the field obscured to minimize macular stimulation. Spectroradiographic measurements were made before and after each session to ensure stimulus quality (SI Appendix, Table S1).

On each of many trials, the participant viewed a pulsed spectral modulation, at one of three contrast levels, designed to target melanopsin, the cones, or both (Fig. 1C). The transition from the background to the stimulation spectrum (melanopsin, cones, or light flux) and the subsequent return

to the background were windowed with a 500-ms half cosine. The total duration of the pulse was 4 s, after which the stimulus field returned to and remained at the background spectrum (Fig. 1D). Twelve seconds after the pulse ended, participants were prompted by an auditory cue to verbally rate their visual discomfort on a 0 to 10 scale. Participants viewed the stimuli through their pharmacologically dilated right eye and a 6-mm-diameter artificial pupil to control retinal irradiance. Infrared video recording of the left eye measured the consensual pupil response during each trial. Each participant viewed at least 12 trials for each crossing of photoreceptor target and contrast, and at least 6 of those trials were required to possess good-quality pupillometry for the subject to be included in the study.

Pupil response was quantified for each trial as the mean percent change in pupil area during the period of 0 to 16 s from stimulus onset, relative to the 0.5 s before stimulus onset. We obtained the median pupil and discomfort response across trials within participant and across participants within groups.

We examined the discomfort and pupil data within a two-stage, nonlinear model (Fig. 3A). The response to a stimulus (either discomfort rating or pupil constriction) is given by

$$Response = m \times \log_{10} \left(\sqrt[\alpha]{(\alpha \times C_{Mel})^\beta + C_{Cone}^\beta} \right) + b,$$

where C_{Mel} and C_{Cone} are the contrasts produced upon the melanopsin and cone photoreceptors by a stimulus, and α , β , m , and b are the four parameters of the model. Nonlinear fitting was performed in MATLAB using `fmincon`, and the variability of parameter estimates within each group was obtained by bootstrap resampling of the data across subjects.

This study was preregistered (SI Appendix, Table S2) and approved by the Institutional Review Board of the University of Pennsylvania. All participants provided informed written consent, and all experiments adhered to the tenets of the Declaration of Helsinki.

Detailed methods are described in SI Appendix, SI Text.

Data Availability. The raw data and analysis code are available through GitHub (<https://github.com/gkaguirre/melSquintAnalysis>) (87).

ACKNOWLEDGMENTS. This work was supported by National Eye Institute Grant R01EY024681 (to D.H.B. and G.K.A.) and Core Grant for Vision Research P30 EY001583, National Institute of Neurological Disorders and Stroke Grant R25 NS065745, National Institute on Aging Grant 5T32AG000255-13, and Department of Defense Grant W81XWH-151-0447 (to G.K.A.).

1. K. B. Digre, K. C. Brennan, Shedding light on photophobia. *J. Neuroophthalmol.* **32**, 68–81 (2012).
2. R. Nosedá, R. Burstein, Advances in understanding the mechanisms of migraine-type photophobia. *Curr. Opin. Neurol.* **24**, 197–202 (2011).
3. H. L. Rossi, A. Recober, Photophobia in primary headaches. *Headache* **55**, 600–604 (2015).
4. G. Selby, J. W. Lance, Observations on 500 cases of migraine and allied vascular headache. *J. Neurol. Neurosurg. Psychiatry* **23**, 23–32 (1960).
5. P. D. Drummond, A quantitative assessment of photophobia in migraine and tension headache. *Headache* **26**, 465–469 (1986).
6. B. K. Rasmussen, R. Jensen, J. Olesen, A population-based analysis of the diagnostic criteria of the International Headache Society. *Cephalalgia* **11**, 129–134 (1991).
7. S. Munjal *et al.*, Most bothersome symptom in persons with migraine: Results from the migraine in America symptoms and treatment (MAST) study. *Headache* **60**, 416–429 (2020).
8. A. Main, A. Dowson, M. Gross, Photophobia and phonophobia in migraineurs between attacks. *Headache* **37**, 492–495 (1997).
9. J. Vanagaite *et al.*, Light-induced discomfort and pain in migraine. *Cephalalgia* **17**, 733–741 (1997).
10. J. V. Vingen, T. Sand, L. J. Stovner, Sensitivity to various stimuli in primary headaches: A questionnaire study. *Headache* **39**, 552–558 (1999).
11. P. A. Kowacs *et al.*, Influence of intense light stimulation on trigeminal and cervical pain perception thresholds. *Cephalalgia* **21**, 184–188 (2001).
12. I. Provencio *et al.*, A novel human opsin in the inner retina. *J. Neurosci.* **20**, 600–605 (2000).
13. D. M. Dacey *et al.*, Melanopsin-expressing ganglion cells in primate retina signal colour and irradiance and project to the LGN. *Nature* **433**, 749–754 (2005).
14. R. Nosedá *et al.*, A neural mechanism for exacerbation of headache by light. *Nat. Neurosci.* **13**, 239–245 (2010).
15. D. M. Berson, Phototransduction by retinal ganglion cells that set the circadian clock. *Science* **295**, 1070–1073 (2002).
16. K. Thapan, J. Arendt, D. J. Skene, An action spectrum for melatonin suppression: Evidence for a novel non-rod, non-cone photoreceptor system in humans. *J. Physiol.* **535**, 261–267 (2001).
17. R. J. Lucas *et al.*, Diminished pupillary light reflex at high irradiances in melanopsin-knockout mice. *Science* **299**, 245–247 (2003).
18. R. J. Lucas, R. H. Douglas, R. G. Foster, Characterization of an ocular photopigment capable of driving pupillary constriction in mice. *Nat. Neurosci.* **4**, 621–626 (2001).
19. P. D. R. Gamlin *et al.*, Human and macaque pupil responses driven by melanopsin-containing retinal ganglion cells. *Vision Res.* **47**, 946–954 (2007).
20. J. M. Stringham, K. Fuld, A. J. Wenzel, Action spectrum for photophobia. *J. Opt. Soc. Am. A Opt. Image Sci. Vis.* **20**, 1852–1858 (2003).
21. J. A. Perez-Leon, E. J. Warren, C. N. Allen, D. W. Robinson, R. L. Brown, Synaptic inputs to retinal ganglion cells that set the circadian clock. *Eur. J. Neurosci.* **24**, 1117–1123 (2006).
22. K. Y. Wong, F. A. Dunn, D. M. Graham, D. M. Berson, Synaptic influences on rat ganglion-cell photoreceptors. *J. Physiol.* **582**, 279–296 (2007).
23. S. Weng, M. E. Estevez, D. M. Berson, Mouse ganglion-cell photoreceptors are driven by the most sensitive rod pathway and by both types of cones. *PLoS One* **8**, e66480 (2013).
24. M. Spitschan, S. Jain, D. H. Brainard, G. K. Aguirre, Opponent melanopsin and S-cone signals in the human pupillary light response. *Proc. Natl. Acad. Sci. U.S.A.* **111**, 15568–15572 (2014).
25. H. McAdams, A. Igdalova, M. Spitschan, D. H. Brainard, G. K. Aguirre, Pulses of melanopsin-directed contrast produce highly reproducible pupil responses that are insensitive to a change in background radiance. *Invest. Ophthalmol. Vis. Sci.* **59**, 5615–5626 (2018).
26. R. B. Lipton, M. E. Bigal, Migraine: Epidemiology, impact, and risk factors for progression. *Headache* **45** (suppl. 1), S3–S13 (2005).
27. J. Olesen, T. J. Steiner, The international classification of headache disorders, 2nd edn (ICDH-II). *Cephalalgia* **24** (suppl. 1), 9–160 (2004).
28. W. F. Stewart, R. B. Lipton, A. J. Dowson, J. Sawyer, Development and testing of the Migraine Disability Assessment (MIDAS) questionnaire to assess headache-related disability. *Neurology* **56** (6, suppl. 1), S20–S28 (2001).
29. M. Yang, R. Rendas-Baum, S. F. Varon, M. Kosinski, Validation of the Headache Impact Test (HIT-6™) across episodic and chronic migraine. *Cephalalgia* **31**, 357–367 (2011).
30. E. G. Conlon, W. J. Lovegrove, E. Chekaluk, P. E. Pattison, Measuring visual discomfort. *Vis. Cogn.* **6**, 637–663 (1999).

31. L. Bossini *et al.*, Sensibilità alla luce e psicopatologia: Validazione del Questionario per la Valutazione della Fotosensibilità (Q.V.F.). *Med. Psicosom.* **51**, 167–176 (2006).
32. J. A. Horne, O. Ostberg, A self-assessment questionnaire to determine morningness-eveningness in human circadian rhythms. *Int. J. Chronobiol.* **4**, 97–110 (1976).
33. N. E. Rosenthal, G. H. Bradt, T. A. Wehr, *Seasonal Pattern Assessment Questionnaire*, (National Institute of Mental Health, Washington DC, 1987).
34. A. Matynia *et al.*, Peripheral sensory neurons expressing melanopsin respond to light. *Front. Neural Circuits* **10**, 60 (2016).
35. R. N. Shepard, Toward a universal law of generalization for psychological science. *Science* **237**, 1317–1323 (1987).
36. R. F. Quick Jr., A vector-magnitude model of contrast detection. *Kybernetik* **16**, 65–67 (1974).
37. A. J. Zele, P. Adhikari, D. Cao, B. Feigl, Melanopsin and cone photoreceptor inputs to the afferent pupil light response. *Front. Neurol.* **10**, 529 (2019).
38. S. B. Baver, G. E. Pickard, P. J. Sollars, G. E. Pickard, Two types of melanopsin retinal ganglion cell differentially innervate the hypothalamic suprachiasmatic nucleus and the olivary pretectal nucleus. *Eur. J. Neurosci.* **27**, 1763–1770 (2008).
39. S. Hattar, H. W. Liao, M. Takao, D. M. Berson, K. W. Yau, Melanopsin-containing retinal ganglion cells: Architecture, projections, and intrinsic photosensitivity. *Science* **295**, 1065–1070 (2002).
40. X. Zhao, B. K. Stafford, A. L. Godin, W. M. King, K. Y. Wong, Photoresponse diversity among the five types of intrinsically photosensitive retinal ganglion cells. *J. Physiol.* **592**, 1619–1636 (2014).
41. U. Grünert, P. R. Jusuf, S. C. S. Lee, D. T. Nguyen, Bipolar input to melanopsin containing ganglion cells in primate retina. *Vis. Neurosci.* **28**, 39–50 (2011).
42. S. Neumann, S. Haverkamp, O. N. Auferkorte, Intrinsically photosensitive ganglion cells of the primate retina express distinct combinations of inhibitory neurotransmitter receptors. *Neuroscience* **199**, 24–31 (2011).
43. P. R. Jusuf, S. C. S. Lee, J. Hannibal, U. Grünert, Characterization and synaptic connectivity of melanopsin-containing ganglion cells in the primate retina. *Eur. J. Neurosci.* **26**, 2906–2921 (2007).
44. J. Hannibal, A. T. Christiansen, S. Heegaard, J. Fahrenkrug, J. F. Kiilgaard, Melanopsin expressing human retinal ganglion cells: Subtypes, distribution, and intraretinal connectivity. *J. Comp. Neurol.* **525**, 1934–1961 (2017).
45. J. Hannibal *et al.*, Melanopsin is expressed in PACAP-containing retinal ganglion cells of the human retinohypothalamic tract. *Invest. Ophthalmol. Vis. Sci.* **45**, 4202–4209 (2004).
46. S. K. Chen, T. C. Badaea, S. Hattar, Photoentrainment and pupillary light reflex are mediated by distinct populations of ipRGCs. *Nature* **476**, 92–95 (2011).
47. P. A. Barrionuevo *et al.*, Assessing rod, cone, and melanopsin contributions to human pupil flicker responses. *Invest. Ophthalmol. Vis. Sci.* **55**, 719–727 (2014).
48. P. A. Barrionuevo, D. Cao, Luminance and chromatic signals interact differently with melanopsin activation to control the pupil light response. *J. Vis.* **16**, 29 (2016).
49. M. Spitschan *et al.*, The human visual cortex response to melanopsin-directed stimulation is accompanied by a distinct perceptual experience. *Proc. Natl. Acad. Sci. U.S.A.* **114**, 12291–12296 (2017).
50. T. M. Brown *et al.*, Melanopsin-based brightness discrimination in mice and humans. *Curr. Biol.* **22**, 1134–1141 (2012).
51. M. Yamakawa, S. I. Tsujimura, K. Okajima, A quantitative analysis of the contribution of melanopsin to brightness perception. *Sci. Rep.* **9**, 7568 (2019).
52. T. DeLawyer, S. I. Tsujimura, K. Shinomori, Relative contributions of melanopsin to brightness discrimination when hue and luminance also vary. *J. Opt. Soc. Am. A Opt. Image Sci. Vis.* **37**, A81–A88 (2020).
53. A. J. Zele, P. Adhikari, B. Feigl, D. Cao, Cone and melanopsin contributions to human brightness estimation. *J. Opt. Soc. Am. A Opt. Image Sci. Vis.* **35**, B19–B25 (2018).
54. R. Storchi *et al.*, Melanopsin-driven increases in maintained activity enhance thalamic visual response reliability across a simulated dawn. *Proc. Natl. Acad. Sci. U.S.A.* **112**, E5734–E5743 (2015).
55. M. Hatori *et al.*, Inducible ablation of melanopsin-expressing retinal ganglion cells reveals their central role in non-image forming visual responses. *PLoS One* **3**, e2451 (2008).
56. R. J. Lucas, Diminished pupillary light reflex at high irradiances in melanopsin-knockout mice. *Science* **299**, 245–247 (2003).
57. M. Cambron, H. Maertens, K. Paemeleire, L. Crevits, Autonomic function in migraine patients: Ictal and interictal pupillometry. *Headache* **54**, 655–662 (2014).
58. D. E. Harle, J. S. Wolffsohn, B. J. W. Evans, The pupillary light reflex in migraine. *Ophthalmic Physiol. Opt.* **25**, 240–245 (2005).
59. O. E. Eren, R. Ruscheweyh, C. Schankin, F. Schöberl, A. Straube, The cold pressor test in interictal migraine patients—different parasympathetic pupillary response indicates dysbalance of the cranial autonomic nervous system. *BMC Neurol.* **18**, 41 (2018).
60. P. D. Drummond, Pupil diameter in migraine and tension headache. *J. Neurol. Neurosurg. Psychiatry* **50**, 228–230 (1987).
61. M. M. Cortez, N. A. Rea, L. A. Hunter, K. B. Digre, K. C. Brennan, Altered pupillary light response scales with disease severity in migrainous photophobia. *Cephalalgia* **37**, 801–811 (2017).
62. M. M. Cortez, N. Rae, L. Millsap, N. McKean, K. C. Brennan, Pupil cycle time distinguishes migraineurs from subjects without headache. *Front. Neurol.* **10**, 478 (2019).
63. K. A. Roeklein *et al.*, Melanopsin gene variations interact with season to predict sleep onset and chronotype. *Chronobiol. Int.* **29**, 1036–1047 (2012).
64. K. A. Roeklein *et al.*, A missense variant (P10L) of the melanopsin (OPN4) gene in seasonal affective disorder. *J. Affect. Disord.* **114**, 279–285 (2009).
65. K. A. Roeklein *et al.*, Melanopsin, photosensitive ganglion cells, and seasonal affective disorder. *Neurosci. Biobehav. Rev.* **37**, 229–239 (2013).
66. J. Johnson *et al.*, Melanopsin-dependent light avoidance in neonatal mice. *Proc. Natl. Acad. Sci. U.S.A.* **107**, 17374–17378 (2010).
67. A. Routtenberg, M. Strop, J. Jerdan, Response of the infant rat to light prior to eyelid opening: Mediation by the superior colliculus. *Dev. Psychobiol.* **11**, 469–478 (1978).
68. D. S. McNeill *et al.*, Development of melanopsin-based irradiance detecting circuitry. *Neural Dev.* **6**, 8 (2011).
69. P. J. Goatsby *et al.*, Pathophysiology of migraine: A disorder of sensory processing. *Physiol. Rev.* **97**, 553–622 (2017).
70. W. M. Mulleners, E. P. Chronicle, J. E. Palmer, P. J. Koehler, J. W. Vredeveld, Visual cortex excitability in migraine with and without aura. *Headache* **41**, 565–572 (2001).
71. D. J. Hodkinson *et al.*, Increased amplitude of thalamocortical low-frequency oscillations in patients with migraine. *J. Neurosci.* **36**, 8026–8036 (2016).
72. V. Marek *et al.*, Implication of melanopsin and trigeminal neural pathways in blue light photosensitivity *in vivo*. *Front. Neurosci.* **13**, 497 (2019).
73. K. Okamoto, R. Thompson, A. Tashiro, Z. Chang, D. A. Bereiter, Bright light produces Fos-positive neurons in caudal trigeminal brainstem. *Neuroscience* **160**, 858–864 (2009).
74. K. Okamoto, A. Tashiro, Z. Chang, D. A. Bereiter, Bright light activates a trigeminal nociceptive pathway. *Pain* **149**, 235–242 (2010).
75. P. D. Drummond, A. Woodhouse, Painful stimulation of the forehead increases photophobia in migraine sufferers. *Cephalalgia* **13**, 321–324 (1993).
76. A. Matynia *et al.*, Light aversion and corneal mechanical sensitivity are altered by intrinsically photosensitive retinal ganglion cells in a mouse model of corneal surface damage. *Exp. Eye Res.* **137**, 57–62 (2015).
77. E. A. Kaiser, A. F. Russo, CGRP and migraine: Could PACAP play a role too? *Neuropeptides* **47**, 451–461 (2013).
78. R. Nosedá *et al.*, Migraine photophobia originating in cone-driven retinal pathways. *Brain* **139**, 1971–1986 (2016).
79. C. A. Bernstein *et al.*, The migraine eye: Distinct rod-driven retinal pathways' response to dim light challenges the visual cortex hyperexcitability theory. *Pain* **160**, 569–578 (2019).
80. O. A. Mahroo, Pupil area and photopigment spectral sensitivity are relevant to study of migraine photophobia. *Brain* **140**, e2 (2017).
81. K. Y. Wong, A retinal ganglion cell that can signal irradiance continuously for 10 hours. *J. Neurosci.* **32**, 11478–11485 (2012).
82. S. K. Lee, T. Sonoda, T. M. Schmidt, M1 intrinsically photosensitive retinal ganglion cells integrate rod and melanopsin inputs to signal in low light. *Cell Rep.* **29**, 3349–3355.e2 (2019).
83. A. Tikidji-Hamburyan *et al.*, Rods progressively escape saturation to drive visual responses in daylight conditions. *Nat. Commun.* **8**, 1813 (2017).
84. E. A. Kaiser, A. Igdalova, G. K. Aguirre, B. Cucchiara, A web-based, branching logic questionnaire for the automated classification of migraine. *Cephalalgia* **39**, 1257–1266 (2019).
85. J. Y. Choi *et al.*, Usefulness of a photophobia questionnaire in patients with migraine. *Cephalalgia* **29**, 953–959 (2009).
86. O. Estévez, H. Spekreijse, The “silent substitution” method in visual research. *Vision Res.* **22**, 681–691 (1982).
87. H. McAdams, G. Frazzetta, G. Aguirre, Analysis code for pupil tracking data for the OLApproach_Squint project. GitHub. <https://github.com/gkaguirrelab/melSquintAnalysis>. Deposited 3 June 2020.

Supplemental Methods

We used silent substitution to create stimuli designed to selectively target melanopsin, the cones, or both (Figure 1c). We presented 4 second pulses of these stimuli to participants and asked them to verbally report the degree of discomfort they experienced while simultaneous pupillometry was recorded (Figure 1d,e).

Participants

A total of 60 participants between the ages of 25 and 40 were recruited from the greater Philadelphia area and University of Pennsylvania campus, in most cases using advertising on digital social media services. All candidate participants underwent screening using the Penn Online Evaluation of Migraine (1), which implements automated headache symptom classification using the International Classification of Headache Disorders (ICHD)-3-beta criteria. The POEM also incorporates a set of previously published questions regarding photophobia during and between headache. These responses were scored with a point for each yes response to questions 1 through 7 (referred to here as the Choi score) (2). Potential participants also completed the Visual Discomfort Score (VDS) survey (3). The VDS score was derived as the sum of scores from 23 questions regarding frequency of particular visual discomfort symptoms, each scored on a 0-3 scale from “never” to “almost always”. To be eligible for the study, potential participants were required to meet all inclusion criteria for one of three groups:

- 1) Migraine with visual aura (MwA): a) classification of migraine with visual aura by the POEM, b) Choi score of 6 or 7, c) a response of “yes” to the Choi query regarding the presence of photophobia during headache free periods, d) one or more headaches within the prior month.
- 2) Migraine without aura (MwoA): a) classification of migraine without aura by the POEM, b) Choi score of 6 or 7, c) a response of “yes” to the Choi query regarding the presence of photophobia during headache free periods, d) one or more headaches within the prior month.
- 3) Control: a) classification of mild non-migrainous headache or headache-free by the POEM, b) a response of “No” or “I don’t know” to a question regarding a family history of migraine, c) a response of “No” to a question regarding a history of childhood motion sickness, d) VDS score 7 or lower.

Exclusion criteria were a history of glaucoma, generalized epilepsy, a history of adverse reaction to dilating eye drops, a concussion in the last six months, ongoing symptoms from head trauma/concussion, best-corrected distance acuity below 20/40 assessed via Snellen eye chart, or abnormal color vision as assessed via Ishihara plates. Participants were not excluded based on medication use, including migraine preventive medications, and were allowed to continue to take their current medications during data collection. We did not explicitly screen control subjects for the possibility that they have migrainous aura unaccompanied by headache. Given the low prevalence of this condition (<0.2%), however, it is unlikely that a participant with this condition is present within the control group (4).

An inability to collect usable pupillometry from a participant was an additional exclusion criterion. Candidate participants were studied in the lab during a pupillometry screening

session that mimicked a subset of trials from the main experiment. To pass this screening session, participants were required to provide acceptable pupillometry data on at least 9 of 12 trials. We screened 83 participants, and 2 were excluded on the basis of this screening criterion. Drawing from the 81 participants who met the pupillometry screening criterion, we ultimately collected archival data on 60 participants, with 20 participants from each group (MwA, MwoA, and controls). Of the remaining 21 participants, 15 either did not respond to subsequent attempts to enroll in the study or were screened after data collection had completed. An additional 6 participants participated in at least one session but failed to return for subsequent sessions.

Stimuli

We designed stimuli that target specific photoreceptor classes through the technique of silent substitution (5). In this approach, sets of light spectra are created that have the property of producing equal excitation of one or more “silenced” classes of photoreceptors, but producing varying excitation on one or more “targeted” photoreceptors. We targeted three main photoreceptor mechanisms: melanopsin, the cones, or both (Figure 1c). We use here the term “light flux” to describe the latter combined stimulus, although we note that our stimulus modulation is not simply a multiplicative scaling of the spectrum, which is what is usually implied by the term.

In prior work we have shown that these different classes of stimuli evoke differential pupil responses (6, 7), evoke visual cortex responses (8), and produce different visual experiences in the observer. In particular, the melanopsin-directed stimulus is described as an uncomfortable brightness (8).

These stimuli were generated in the same manner as described in prior reports (8, 9). Briefly, we used a digital light synthesis engine (OneLight Spectra, Vancouver, BC, Canada) that produces stimulus spectra as mixtures of 56 independent primaries (~16 nm full width at half maximum) under digital control and can modulate between these spectra at 256 Hz. We tailored the photoreceptor spectral sensitivities for each individual observer, taking into account the participant’s age, pupil size, and our field size of 27.5 degrees (Figure 1f). Cone fundamentals were based on the International Commission on Illumination (CIE) physiological cone fundamentals (10). The CIE standard only specifies fundamentals up to field sizes of 10 degrees, so we obtain estimates for our 27.5 degree field by extrapolating the formula using the open-source Psychophysics Toolbox (11–13). We created separate background and stimulation spectra that provided 1) a nominal 400% unipolar Weber contrast on melanopsin while silencing the cones for our melanopsin-directed background/stimulus pair (melanopsin direction), 2) 400% contrast on each L-, M-, and S-cone classes while silencing melanopsin for the cone-directed modulation/stimulus pair (cones direction), and 3) 400% contrast each on melanopsin and each L-, M-, and S-cone classes for the light flux modulation/stimulus pair (light flux direction) (Figure 1c). The background spectra for each stimulus type differed in background luminance, but had similar chromaticity (Supplementary Table 1) as calculated using the XYZ functions associated with the CIE 2006 10-degree cone fundamentals (<http://www.crvl.org>) (10). We also produced contrast levels of 100 and 200% for each stimulus direction by scaling the relevant stimulus spectrum. We did not explicitly silence

rods or penumbral cones (9), although we believe that the luminance and temporal properties of our stimuli minimize the contribution of these photoreceptors.

Stimuli were presented through a custom-made eyepiece with a circular, uniform field of 27.5° diameter. The central 5° diameter of the field was obscured to block the effects of the foveal macular pigment which can cause variation in photoreceptor spectral sensitivity (Figure 1f).

We obtained 5 spectroradiometric measurements of the 400% stimuli and their backgrounds before and after each testing session. For each stimulus type, we determined contrast on the following post-receptoral mechanisms: LMS, L-M, S, and melanopsin. Supplementary Table 1 presents the average validation results across all sessions. The validation results for each session are included with the experimental data for download. We adjusted our apparatus over the duration of data collection to maintain the luminance of the background spectrum for the light flux stimulus between 160 and 254 cd/m².

We discarded data from a session if the post-experiment stimulus validation measurements did not meet our pre-registered criteria. Data were discarded if the median of the 5 post-experiment measurements was: 1) greater than 20% absolute contrast on any of the nominally silenced post-receptoral mechanisms; or 2) less than 350% contrast upon a targeted post-receptoral mechanism. In the event that data from a session were discarded, the session was repeated at a later date. Prior to starting a data collection session, pre-experiment stimulus validation measurements were required to meet these same criteria.

Experiment Structure

Participants were studied during multiple data collection sessions, usually held on different days, in an attempt to minimize fatigue during any one session. In an attempt to minimize variation in circadian cycle across sessions, subsequent sessions were initiated within three hours of the time of day when the same participant started their first session.

Participants were exposed to similar “light history” prior to data collection. At the start of a session, participants entered the testing room and underwent pharmacologic dilation of their right eye with 0.5% proparacaine for anesthesia and then 1% tropicamide ophthalmic solution. Participants remained in the testing room for the next 20 minutes, receiving instructions and adjusting the position of the apparatus for comfort. Room lights were set so that the walls of the testing room had a measured luminance of ~150 cd/m², equated to the background luminance of our light flux stimulus. After confirming the presence of pupil dilation, the room lights were turned off and a curtain closed behind the participant to block light from the screen of the computer that controlled the apparatus. Apart from the light from the eyepiece, the participant remained in darkness for the remainder of the experiment. Participants viewed the stimuli through their pharmacologically dilated right eye and a 6 mm diameter artificial pupil to control retinal irradiance.

On each of many trials, the participant viewed a pulsed spectral modulation designed to target melanopsin, the cones, or both (Figure 1c). The transition from the background to the stimulation spectrum (melanopsin, cones, or light flux) and the subsequent return to

the background were windowed with a 500 ms half-cosine. This step minimized the entopic percept of a Purkinje tree in the melanopsin-directed stimulus (9). The total duration of the pulse was 4 seconds, after which the stimulus field returned to and remained at the background spectrum (Figure 1d). Twelve seconds after the pulse ended, participants were prompted by an auditory cue to verbally report their discomfort rating (described below). This verbal rating was recorded by a microphone during the 4 second response window, the end of which was marked by another auditory cue. There was a variable inter-trial-interval of 1.5 – 2.5 seconds (uniformly distributed) that reduced the predictability of the onset of the next trial.

Ten consecutive trials that targeted the same photoreceptor direction but varied in contrast were grouped together into an acquisition. The ordering of the contrast levels (100, 200, 400%) followed a counterbalanced sequence to avoid trial order effects (14); the first trial was discarded so that all retained trials had controlled first-order stimulus history. A total of 6 acquisitions, 2 of each stimulus type, comprised a single session. Acquisitions were ordered such that consecutive acquisitions were not of the same stimulus class. Data collection for a participant was deemed sufficient when a subject had completed two sessions, and these sessions contained in total at least six acceptable trials—as judged by pupillometry—for each stimulus type. Only acceptable trials were included in pupillometry analysis, but all trials were included in analysis of discomfort ratings. We attempted to gather 4 sessions of data for each individual participant but retained all subjects with data collection that was deemed sufficient. Participants did not complete all 4 sessions for a variety of reasons, including failure of post-experiment stimulus validation, poor pupillometry requiring us to discard that session, or declining to return for subsequent sessions. Across all 60 participants, 45 completed 4 sessions (15 controls, 15 M_wA, 15 M_woA), 11 completed 3 sessions (4 controls, 3 M_wA, 4 M_woA), and 4 completed 2 sessions (1 control, 2 M_wA, 1 M_woA).

Discomfort Ratings

At the end of each trial, participants were asked to rate the discomfort produced by the stimulus on a 0 – 10 scale. The experimenter read this prompt to the participant at the start of each session:

“Following each trial, please rate the degree of discomfort that you experienced from the light pulse on a scale of zero to ten. A score of zero means that the pulse was not at all uncomfortable. A score of five means that the light pulse was moderately uncomfortable. A score of ten means that the light pulse was extremely uncomfortable.”

Following completion of the experiment, raters masked to group assignment manually transcribed these verbal discomfort ratings. Trials on which no rating was given, or on which the spoken rating was un-interpretable, were discarded.

Pupillometry

We recorded the consensual pupil response from the left eye of the participant (contralateral to the eye receiving the stimulus) using an infrared camera (Pupil Labs GmbH) mounted on a post ~25 mm from the eye. A video clip was recorded for each trial, starting 1.5-s prior to pulse onset and ending 12-s after pulse offset (Figure 1d,e). These videos were processed using custom software

(<https://github.com/gkaguirrelab/transparentTrack>) (15) to fit an ellipse to the identified pupil boundary in each video frame, allowing us to extract pupil area over time.

This raw pupillometry data underwent several stages of pre-processing to remove and interpolate over frames in which the pupil had been poorly identified. The first stage involves blink censoring, which was performed by identifying frames in which the glint from the active infrared light source of the camera was absent. Several frames before and after each blink were also censored to remove blink-related artifacts, with these values adjusted on a per-participant basis. Next, frames in which the pupil was identified but poorly fit by the routine were censored. This step largely functioned to remove frames in which much of the pupil was obscured by the eyelid. Lastly, frames in which the identified pupil was implausibly large or small were removed. Linear interpolation was performed over censored frames. If more than 25% of frames in a given trial were censored that trial was discarded from analysis. Pupil responses were expressed as the percentage change in area relative to the 0.5-s prior to the stimulus onset.

Six participants had frequent, brief blinks that produced many missed frames of pupil tracking despite having video recording of the eye that was otherwise of good quality. The data from these participants were retained despite having more than 25% missing frames in a trial.

All manual adjustment of pupillometry, and indeed the development of the processing steps and criteria, was performed by investigators masked to the group membership of the participants.

Analysis

Data analysis was performed using custom MATLAB code (Mathworks). We used a one-way ANOVA to determine the effect of group upon the clinical and demographic measures. Significant effects were examined in post-hoc testing using the Tukey procedure.

We took the median of discomfort rating across trials within a participant, and the mean across participants within a group. Pupil response was quantified for each trial as the mean percent change in pupil area during the period of 0 to 16 seconds from stimulus onset, relative to the 0.5 seconds before stimulus onset. The mean response across trials within participant, and across participants within groups, was obtained.

We examined the discomfort and pupil data within a two stage, non-linear model (Figure 3a). The response to a stimulus (either discomfort rating or pupil constriction) is given by:

$$Response = m * \log_{10} \left(\sqrt[\beta]{(\alpha * C_{Mel})^\beta + C_{Cone}^\beta} \right) + b$$

where C_{Mel} and C_{Cone} are the contrasts produced upon the melanopsin and cone photoreceptors by a stimulus, and α , β , m , and b are the four parameters of the model.

The first two model parameters describe an initial, non-linear stage that combines the photoreceptor contrast inputs and provides an “ipRGC contrast” output. The melanopsin contrast (α) is weighted by the first parameter, and then the weighted melanopsin contrast and the cone contrast are then combined using the Minkowski distance metric, with the second parameter (β) being the exponent for the metric. The modeled ipRGC contrasts of the stimuli are then base-10 log transformed and passed through a two-parameter affine transformation (parameters, slope and intercept of the transformation). In reporting the parameters, we convert the intercept parameter to an “offset” value, which is the predicted response amplitude at an ipRGC contrast of 200%.

The model was fit to the mean (across participant) data for all stimuli, with separate models fits performed for each group, and for each data type (discomfort rating and pupil response). Model fitting was performed using the *fmincon* function in MATLAB to minimize the L2 norm between the modeled values and the data. This fitting procedure was repeated over 1000 bootstrap resamples (with replacement) of the participants to assess the variability of the model output. We observed that the β parameter deviated slightly from a normal distribution across bootstraps. Therefore, we obtained the median value for all parameters across bootstraps, and variability across bootstraps was expressed by dividing the inter-quartile range of the values across bootstraps by 1.35, yielding a measure commensurate with the standard deviation of the distribution and thus an estimate of the standard error of the mean of the central tendency of the parameters.

Pre-Registration and availability of data and analysis code

This study was the subject of an initial pre-registration document (<https://osf.io/5ry67/>) and subsequent addenda (project summary page: <https://osf.io/qjxdf/>). Supplementary Table 2 summarizes the pre-registration documents and our deviations from these protocols. The analysis code and data are available (<https://github.com/gkaguirrelab/melSquintAnalysis>).

Supplementary Tables

Stimulus	Contrast				Luminance [cd/m ²]	Chromaticity [x, y]
	<i>Melanopsin</i>	<i>LMS</i>	<i>S</i>	<i>L-M</i>		
Mean stimulus values across subjects						
<i>Mel</i>	397.06%	0.40%	-0.06%	-0.87%	322	0.58, 0.38
<i>Cones</i>	0.83%	397.72%	1.72%	1.02%	145	0.57, 0.36
<i>LF</i>	398.74%	399.41%	-2.09%	-0.08%	209	0.57, 0.36
Mean unsigned contrast error across subjects						
<i>Mel</i>	4.05%	0.51%	1.26%	0.87%	-	-
<i>Cones</i>	0.86%	2.32%	4.66%	1.05%	-	-
<i>LF</i>	1.42%	1.27%	3.33%	0.41%	-	-

Supplementary Table 1. Stimulus Validation Measurements. Before and after each experiment, we obtained 5 spectroradiographic measurements of each stimulus at its background and maximal (400% nominal) contrast level. From these measurements, we calculated the contrast on several receptor and post-receptoral mechanisms: melanopsin, the combined luminance channel (LMS), S-(L+M), and L-M. We also measured the luminance and chromaticity of the background spectrum for each stimulus. The upper portion of the table provides the mean of these validation measurements across sessions and subjects. The lower portion of the table presents the mean (across sessions and subjects) unsigned deviation of the validated stimuli from the nominal contrast levels.

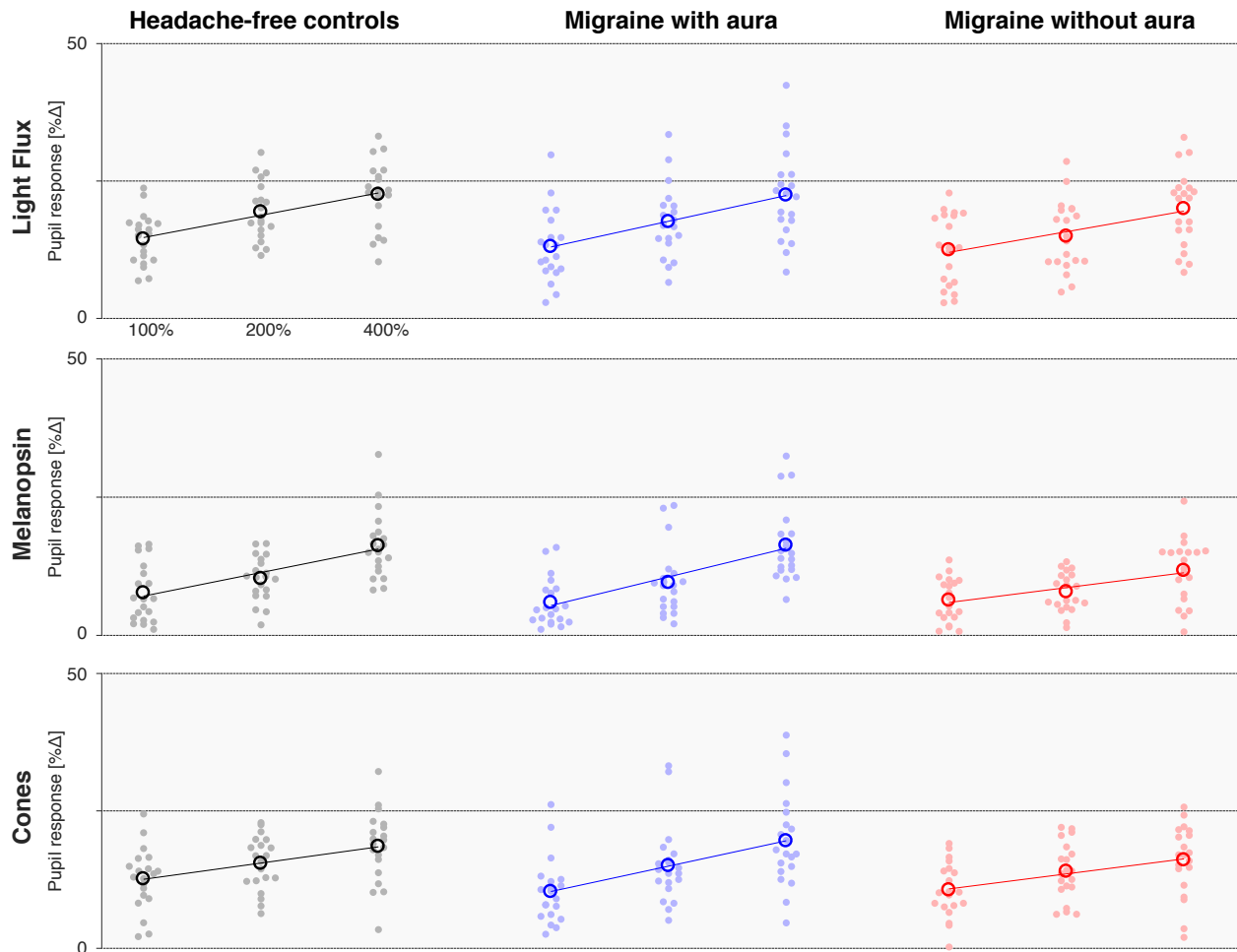
Stimulus	Group comparison	Mean discomfort difference	t-statistic	p-value
Melanopsin	MwA - Controls	1.558	3.719	*1.314e-03
	MwoA - Controls	1.717	4.097	*3.889e-04
	MwoA - MwA	0.158	0.378	9.24E-01
Cones	MwA - Controls	1.675	3.321	*4.403e-03
	MwoA - Controls	1.983	3.933	*6.648e-04
	MwoA - MwA	0.308	0.611	8.15E-01
Light Flux	MwA - Controls	1.975	3.486	*2.697e-03
	MwoA - Controls	2.258	3.986	*5.594e-04
	MwoA - MwA	0.283	0.500	8.72E-01

Supplementary Table 2. ANOVA result. We examined the effect of group and stimulus upon mean discomfort ratings using a two-way, mixed effects ANOVA. Independent variables included group (migraine with aura, without aura, and control) as a between subjects factor and photoreceptor target (melanopsin, cones, and light flux) as a within subjects factor. Post-hoc testing was conducted using the Tukey procedure.

Type	Link	Contents
Initial pre-registration	https://osf.io/5ry67/	<ul style="list-style-type: none"> - Defined initial plan for experiment, including subject recruitment, screening procedure, stimulus creation, experimental design, exclusion criteria, and primary analyses.
Addendum #1	https://osf.io/qtjyd/	<ul style="list-style-type: none"> - Modified subject exclusion criteria to exclude subjects with a history of ophthalmologic disease. - Modified subject exclusion criteria to exclude candidate migraine participants who had not experienced a headache within the previous month. Seven migraine subjects with no headache in the prior month were enrolled in the study prior to the adoption of this criterion and are included in the resulting data set. - Defined a specific target range for the luminance of the background stimulus spectrum. - Added '<i>Morningness-Eveningness Questionnaire</i>'. - Added a procedure to ask subjects in the week after a session if they have experienced a migraine since their participation in a session.
Addendum #2	https://osf.io/kf253/	<ul style="list-style-type: none"> - Defined a procedure to perform an examination of the pupil response data, masked to group assignment, to inform a revision of subject recruitment targets.
Addendum #3	https://osf.io/j3x24/	<ul style="list-style-type: none"> - Revised recruitment goal to 20 subjects within each group from the original target of 40.
Deviations		<ul style="list-style-type: none"> - We had proposed to report median values across subjects. Using the median value result in unstable bootstrap model fits due to the discontinuous nature of the discomfort ratings data. We therefore switched to the mean for all across-subject measures.

Supplementary Table 3. Summary of Pre-registrations, addenda, and protocol deviations.

Supplementary Figures



Supplementary Figure 1. Pupil response amplitudes by stimulus and group. Each row presents the mean percent change in pupil area (across the duration of the trial) elicited by stimuli that targeted a particular combination of photoreceptors, and each column contains the data from each individual group ($n = 20$ participant per group). The stimuli were presented at three different contrast levels (100, 200, and 400%), and these values (log-spaced) define the x-axis of each subplot. The mean (across trial) pupil response for a given stimulus and contrast is shown for each participant (filled circle), as is the mean response across participants (open circle). The best fit line to the mean pupil response across participants as a function of log contrast is shown in each subplot.

References

1. E. A. Kaiser, A. Igdalova, G. K. Aguirre, B. Cucchiara, A web-based, branching logic questionnaire for the automated classification of migraine. *Cephalalgia* **39**, 1257–1266 (2019).
2. J. Y. Choi, *et al.*, Usefulness of a photophobia questionnaire in patients with migraine. *Cephalalgia* **29**, 953–959 (2009).
3. E. G. Conlon, W. J. Lovegrove, E. Chekaluk, P. E. Pattison, Measuring visual discomfort. *Vis. cogn.* **6**, 637–663 (1999).
4. M. B. Russell, J. Olesen, A nosographic analysis of the migraine aura in a general population. *Brain* **119**, 355–361 (1996).
5. O. Estévez, H. Spekreijse, The “silent substitution” method in visual research. *Vision Res.* **22**, 681–691 (1982).
6. M. Spitschan, S. Jain, D. H. Brainard, G. K. Aguirre, Opponent melanopsin and S-cone signals in the human pupillary light response. *Proc. Natl. Acad. Sci.* **111**, 15568–15572 (2014).
7. H. McAdams, A. Igdalova, M. Spitschan, D. H. Brainard, G. K. Aguirre, Pulses of melanopsin-directed contrast produce highly reproducible pupil responses that are insensitive to a change in background radiance. *Investig. Ophthalmol. Vis. Sci.* **59**, 5615–5626 (2018).
8. M. Spitschan, *et al.*, The human visual cortex response to melanopsin-directed stimulation is accompanied by a distinct perceptual experience. *Proc. Natl. Acad. Sci.* **114**, 12291–12296 (2017).
9. M. Spitschan, G. K. Aguirre, D. H. Brainard, Selective stimulation of penumbral cones reveals perception in the shadow of retinal blood vessels. *PLoS One* **10** (2015).
10. CIE, Fundamental chromaticity diagram with physiological axes – Part 1. Technical Report 170-1 (Central Bureau of the Commission Internationale de l’Éclairage, Vienna) (2006).
11. M. Kleiner, *et al.*, What’s new in Psychtoolbox-3? *Perception* **36**, 1–16 (2007).
12. D. H. Brainard, The Psychophysics Toolbox. *Spat. Vis.* **10**, 433–436 (1997).
13. D. G. Pelli, The VideoToolbox software for visual psychophysics: Transforming numbers into movies. *Spat. Vis.* **10**, 437–442 (1997).
14. G. K. Aguirre, M. G. Mattar, L. Magis-Weinberg, De Bruijn cycles for neural decoding. *Neuroimage* **56**, 1293–1300 (2011).
15. G. K. Aguirre, A model of the entrance pupil of the human eye. *Sci. Rep.* **9**, 9360 (2019).